http://dx.doi.org/10.5607/en.2014.23.1.53
Exp Neurobiol. 2014 Mar;23(1):53-64.
pISSN 1226-2560 • eISSN 2093-8144

Original Article

Experimental Neurobiology

Attenuated Glial K^+ Clearance Contributes to Long-Term Synaptic Potentiation Via Depolarizing GABA in Dorsal Horn Neurons of Rat Spinal Cord

Jaekwang Lee[1,3], Oleg V Favorov[1], Mark Tommerdahl[1], C. Justin Lee[3,4*] and Barry L. Whitsel[1,2*]

[1]Department of Biomedical Engineering, University of North Carolina at Chapel Hill, Chapel Hill, NC, USA,
[2]Department of Cell and Molecular Physiology, University of North Carolina at Chapel Hill, Chapel Hill, NC, USA,
[3]WCI Center for Functional Connectomics, Institute of Science and Technology (KIST), Seoul, Korea,
[4]KU-KIST Graduate School of Converging Science and Technology, Korea University, Seoul, Korea

It has been reported that long-term enhancement of superficial dorsal horn (DH_s) excitatory synaptic transmission underlies central sensitization, secondary hyperalgesia, and persistent pain. We tested whether impaired clearance of K^+ and glutamate by glia in DH_s may contribute to initiation and maintenance of the CNS pain circuit and sensorimotor abnormalities. Transient exposure of the spinal cord slice to fluorocitrate (FC) is shown to be accompanied by a protracted *decrease* of the DH_s optical response to repetitive electrical stimulation of the ipsilateral dorsal root, and by a similarly protracted *increase* in the postsynaptic response of the DH_s like LTP. It also is shown that LTP_{FC} *does not* occur in the presence of APV, and becomes progressively *smaller* as $[K^+]_o$ in the perfusion solution decreased from 3.0 mM to 0.0 mM. Interestingly LTP_{FC} is *reduced* by bath application of Bic. Whole-cell patch recordings were carried out to evaluate the effects of FC on the response of DH_s neurons to puffer-applied GABA. The observations reveal that transient exposure to FC is reliably accompanied by a prolonged (>1 hr) depolarizing shift of the equilibrium potential for the DH_s neuron transmembrane ionic currents evoked by GABA. Considered collectively, the findings demonstrate that LTP_{FC} involves (1) elevation of $[K^+]_o$ in the DH_s, (2) NMDAR activation, and (3) conversion of the effect of GABA on DH_s neurons from inhibition to excitation. It is proposed that a transient impairment of astrocyte energy production can trigger the cascade of dorsal horn mechanisms that underlies hyperalgesia and persistent pain.

Key words: dorsal horn, astrocytes, glia-neuron interactions, central sensitization, hyperalgesia, persistent pain

INTRODUCTION

Direct application to the spinal cord of a variety of substances (e.g., excitatory neurotransmitters such as substance P or NMDA receptor agonists) or low-frequency nociceptor afferent input can produce a long-term enhancement of excitatory synaptic transmission between C-fiber afferents and neurons in the DH_s [1-3]. Clearly, therefore, establishment of the long-term enhancement

Received March 2, 2014, Revised March 5, 2014,
Accepted March 5, 2014

*To whom correspondence should be addressed.
C. Justin Lee
TEL: 82-2-958-6940, FAX: 82-2-958-6937
e-mail: cjl@kist.re.kr
Barry L. Whitsel
TEL: 1-919-966-1291, FAX: 1-919-966-6927
e-mail: bwhitsel@med.unc.edu

of DH_s excitatory synaptic transmission that underlies central sensitization, secondary hyperalgesia, and persistent pain does not, as previously believed, require a sustained preceding period of high-frequency nociceptor afferent activation.

The experiments described in this paper were motivated by the intriguing and clinically relevant possibility that a long-term enhancement of DH_s excitatory synaptic transmission not only can occur in the absence of a preceding period of conditioning afferent drive (as described above), but can arise subsequent to an impairment of DH_s glial energy metabolism. Observations reported in previous studies are fully consistent with the idea that impairment of the ability of astrocytes to regulate extracellular K^+ and glutamate levels alters excitatory neurotransmission at multiple levels of the CNS. As examples: (1) the secondary hyperalgesia that follows intradermal injection of 5% formalin is accompanied by an impaired ability of astrocytes to regulate $[K^+]_o$ and $[glutamate]_o$ in the region of the DH_s that receives its input from the injected skin site [4, 5], (2) even a brief (40 sec) increase in extracellular K^+ induces LTP in the hippocampal slice [6]; (3) hippocampal LTP is substantially reduced in animals in which astrocytes are rendered unable (via a selective genetic manipulation) to release neurotransmitters [7]; (4) d-serine released from astrocytes is critical for the induction of LTP in hippocampal slices [8]; (4) the slow astrocytic depolarization that accompanies hippocampal LTP is due to astrocyte uptake of K^+ and supports neuronal LTP by reducing the efficacy of astrocytic glutamate transporters and inducing astrocyte release of a variety of signaling molecules (for review see [9]); and, finally, (5) intracerebral injection of fluorocitrate (a reversible, selective inhibitor of glial metabolism, [5, 10]) elevates $[K^+]_o$, increases cortical neuron excitability, and induces focal epileptiform discharge [11].

The goals of this study were to: (1) investigate the possibility that transient impairment of spinal cord glial energy metabolism can, in the absence of a preceding period of conditioning afferent drive, initiate the long-term enhancement of DH_s excitatory synaptic transmission widely regarded to underlie central sensitization, secondary hyperalgesia, and persistent pain [3, 12]; and, (2) acquire information bearing directly on the validity of the recent proposal that impaired astrocytic regulation of $[K^+]_o$ can lead to conversion of the effect of GABA on DH_s neurons from inhibition to excitation [4, 13, 14].

MATERIALS AND METHODS

Experiments were performed in accordance with National Institutes of Health guidelines for animal care and welfare. Protocols were approved in advance by the UNC Institutional Animal Care and Use Committee. Subjects were young adult rats (21~35 days; 50~150 g; Sprague-Dawley, Charles River).

Slice Preparation

Transverse slices of the lumbosacral cord (400~800 μm thickness) were cut using an oscillating tissue slicer (OTS-4000, Electron Microscopy Sciences, Vibratome 3000) and placed in a reservoir containing ACSF warmed (30°C) and oxygenated (using a 95% O_2 and 5% CO_2 gas mix). Slices remained in the reservoir (never less than 1 hr) until transferred by pipette to a submerged position in a recording chamber perfused with warmed (28~30.8°C) and oxygenated ACSF (perfusion rate 2~3 ml/min). Composition (in mM) of the ACSF delivered to the slice prior to treatment with a drug or drug combination was 124 NaCl, 3.0 KCl, 2.5 $CaCl_2$, 25 $NaHCO_3$, 1 $MgSO_4$, 1.25 NaH_2PO_4, and 10 glucose. A total of 22 slices were studied.

The procedure reported by Paulsen et al. (1987) was used to prepare dl-fluorocitric acid (FC; Sigma). The barium salt of FC was dissolved in 0.1 M HCl; 0.1 M Na_2SO_4 was added to precipitate barium, and the solution centrifuged at 800~1,000 g for 5~10 min after buffering with 0.1 M $NaPO_4^-$. The supernatant containing FC then was transferred and added to ACSF to achieve a stock FC concentration of 1 mM. For the experiment the stock solution of 1 mM FC in ACSF was diluted to the desired concentration by adding additional ACSF or, when required, d-2-amino-5-phosphonopentanoic acid (D-APV; Sigma) and/or bicuculline (Bic; Sigma) were added to achieve the desired concentrations of FC and drug or FC + drug-combination in ACSF. After warming and oxygenation drug-containing ACSF was delivered to the submerged slice via the chamber perfusion system. In other experiments the solution used to perfuse the slice was switched to ACSF containing a less-than-normal concentration of K^+ (i.e., 0.0, 1.0, or 2.0 mM rather than 3.0 mM; accomplished by equimolar substitution of NaCl for KCl).

OIS Imaging

The slice was transilluminated and images obtained at ×2 or ×4 magnification using an inverted microscope (Diaphot 200, Nikon) and a cooled, slow-scan CCD camera (Photometrics Inc.). An optical intrinsic signal (OIS_{DR}) was evoked within the DH_s by application of a repetitive constant-current stimulus to the dorsal entry zone using a glass insulated, 50 μm diameter, metal bipolar stimulating electrode connected to an isolation unit, and programmable pulse generator (Master-8, AMPI). Stimulation parameters were: pulse duration - 0.2 ms; intensity - 2~4× the threshold current for evoking an optical response; train duration - 1.0 s; frequency - 20 Hz; intertrain interval - 5 min. Each image

http://dx.doi.org/10.5607/en.2014.23.1.53

included all of the dorsal horn on the same (ipsilateral) side as the stimulated dorsal root, much of the adjacent ventral horn, and a large portion of the bounding white matter. 30 images were obtained in association with each repetitive dorsal root stimulus (a "trial"). The 1st and 2nd images ("reference" images) in each trial were obtained at 1,000 ms and at 500 ms, respectively, prior to stimulus onset; 2 "poststimulus onset" images were acquired during delivery of the repetitive stimulus, and the remaining 26 images after stimulus termination (image acquisition rate=2/s). Trial duration was 9 s.

An average (across-frame) difference image was generated from the optical response to each repetitive dorsal root stimulus by (1) subtracting the reference image obtained at 500 ms before stimulus onset from each image obtained in the same trial between 2.0~7.5 s after stimulus onset (images 6~25; total of 20), and (2) at each pixel location by dividing the sum of the differences between the post-stimulus and reference images (same-trial) by the number of frames. An intensity value was calculated for each pixel in a difference image using the formula $\Sigma(T_{ij}-T_{i,ref})/T_{i,ref}$, where T_{ij} is the intensity of the i^{th} pixel in the j^{th} image, and $T_{i,ref}$ is the intensity of the i^{th} pixel in the reference image. Mean intensity ($\Delta T/T$) of the OIS_{DR} was determined by computing the average intensity of all pixels within the responding region of the horn. The effect on the OIS_{DR} of bath-applied drug (either 50 μM FC or 50 μM APV, or 50 μM FC and 50 μM APV in combination) was expressed as a percentage of the mean intensity of the response observed prior to treatment: i.e., $\Delta T/T_{treatment}/\Delta T/T_{control}\times 100=\%$.

Field potential recording

Single-pulse (0.2 ms) constant-current stimuli were applied to the dorsal root using a suction electrode, isolation unit, and programmable pulse generator (Master 8, AMPI). The population postsynaptic potential evoked by the dorsal root stimulus ($P\text{-}PSP_{DR}$) was recorded with a 1~2 mM NaCl-containing micropipette (1.2 mm OD). All recordings of the $P\text{-}PSP_{DR}$ were obtained from a locus in the substantia gelatinosa (SG) medial to the dorsal root entry zone - at this site the OIS_{DR} is maximal and the recorded field potential consists of both short- and longer-latency responses to single-pulse stimulation of the dorsal root [15-17]. $P\text{-}PSP_{DR}$s were evoked using stimulus intensities 2~4× the minimum ("threshold"; typically 50~80 μA) current required to elicit a $P\text{-}PSP_{DR}$. Such currents activate both large- (A_β) and small-diameter (A_δ and C) afferents in the dorsal root [17-22]. Recordings were filtered (30~300 Hz) and sampled at 50 kHz using pClamp 7.0 (Axon Instruments). Individual field potential recordings were quantified by measuring the baseline-to-peak amplitude between 0~20 ms after stimulus onset; time course of the effect of each experimental manipulation was determined by plotting average evoked potential amplitude vs. time.

Whole cell patch clamp recording

In experiments of this type the slice was transferred from the reservoir to the recording chamber of a fixed-stage upright microscope (Olympus BX51WI) and visualized directly via the microscope's optics, or indirectly via a high resolution CCD camera system (CCD-100, Dage-MTI, Inc) that received the output of a CCD camera attached to the microscope's video port. Whole cell patch-clamp recordings were obtained from lamina II neurons using borosilicate glass pipettes (resistance 4~6 MOhm) pulled on a 2-stage vertical pipette puller (Narishige PC-10), and filled with a solution with the following composition (in mM): 120.0 K-gluconate, 20.0 KCl, 2.0 $NaCl_2$, 20.0 HEPES, 0.5 EGTA, 10.0 glucose, 2.0 Na-ATP, 0.5 Na-GTP; pH adjusted to 7.3 with KOH. Patch recordings were obtained under the same slice conditions (temperature, perfusion rate, etc.) used to obtain OIS imaging and field potentials observations. Voltage-clamp and current-clamp recordings were carried out with a MultiClamp 700B amplifier, using pClamp9 acquisition software (Molecular Devices, Union City, CA, USA). Signals were filtered at 50~500 Hz, sampled at 5 kHz for identification of cell type and at 50 Hz for the GABA application part of the experiment. Data were analyzed and plotted using Origin 7.0. No correction for liquid junction potential was made. Cells with resting potentials greater than -60 mV or less than -80 mV were regarded as "abnormal" and were not studied further.

Once a neuron was accepted for study the tip of a glass pipette filled with 1 mM GABA was placed (using a 3-axis micropositioner; NMN-25, Narishige Group Inc., Tokyo, Japan) at a location within 50~100 μm of the soma. The GABA equilibrium potential (E_{GABA}) was determined by measuring the transmembrane current evoked by a temporally controlled, local application of GABA (a 300 msec "puff" delivered at 3~5 psi via the pipette filled with 1 mM GABA; using Picospritzer II, Parker Hannifin Corp.) at holding potentials ranging between -100 mV and -20 mV (step size=20 mV), both before and after exposure of the slice to FC. Each GABA puff applied during the study of a neuron was delivered at the same location in the DH_s, and at the same pressure and duration.

RESULTS

Population-level observations-

Effects of FC on the OIS_{DR}

In each of 3 slices the OIS_{DR} evoked in the ipsilateral DH_s by

electrical stimulation of the dorsal root was recorded at regular intervals (i) before ("Control"), (ii) throughout a 20 min exposure to ACSF containing 50 μM FC ("FC"), and (iii) during the 60 min period following the restoration of perfusion with drug-free ACSF ("Washout"). Labels in the top left image in Fig. 1A (grayscale) identify the position of the DH_s, the location of the tip of the stimulating electrode (E - in the part of the dorsal root entry zone that overlies the medial half of the DH_s), and the structures which border the DH_s on the left side of the slice (e.g., DC - dorsal column; LC - lateral column; VH - ventral horn). The colour-coded average difference images in Fig. 1A (i.e., average prestimulus - poststimulus images) show that not only did it decrease in both intensity (ΔT/T) and spatial extent during the 20 min exposure to 50 μM FC (FC *vs.* Control images), but it continued to decrease during the 60 min period after the perfusion solution was returned to drug-free ACSF (FC *vs.* Washout images). The across-slice (n = 3) plot of mean ΔT/T *vs.* time in Fig. 1B shows the time course of the effect of FC on the OIS_{DR} (filled circles).

Effects of FC on the P-PSP_{DR}

The superimposed field potential recordings (each trace is the average response to 10 stimulus trials) in Fig. 1C illustrate the effect of FC on the population postsynaptic potential (P-PSP_{DR}) evoked in the ipsilateral DH_s by a single-pulse constant-current stimulus to the attached dorsal root. Note that although for this exemplary slice the P-PSP_{DR} recorded during the exposure to FC

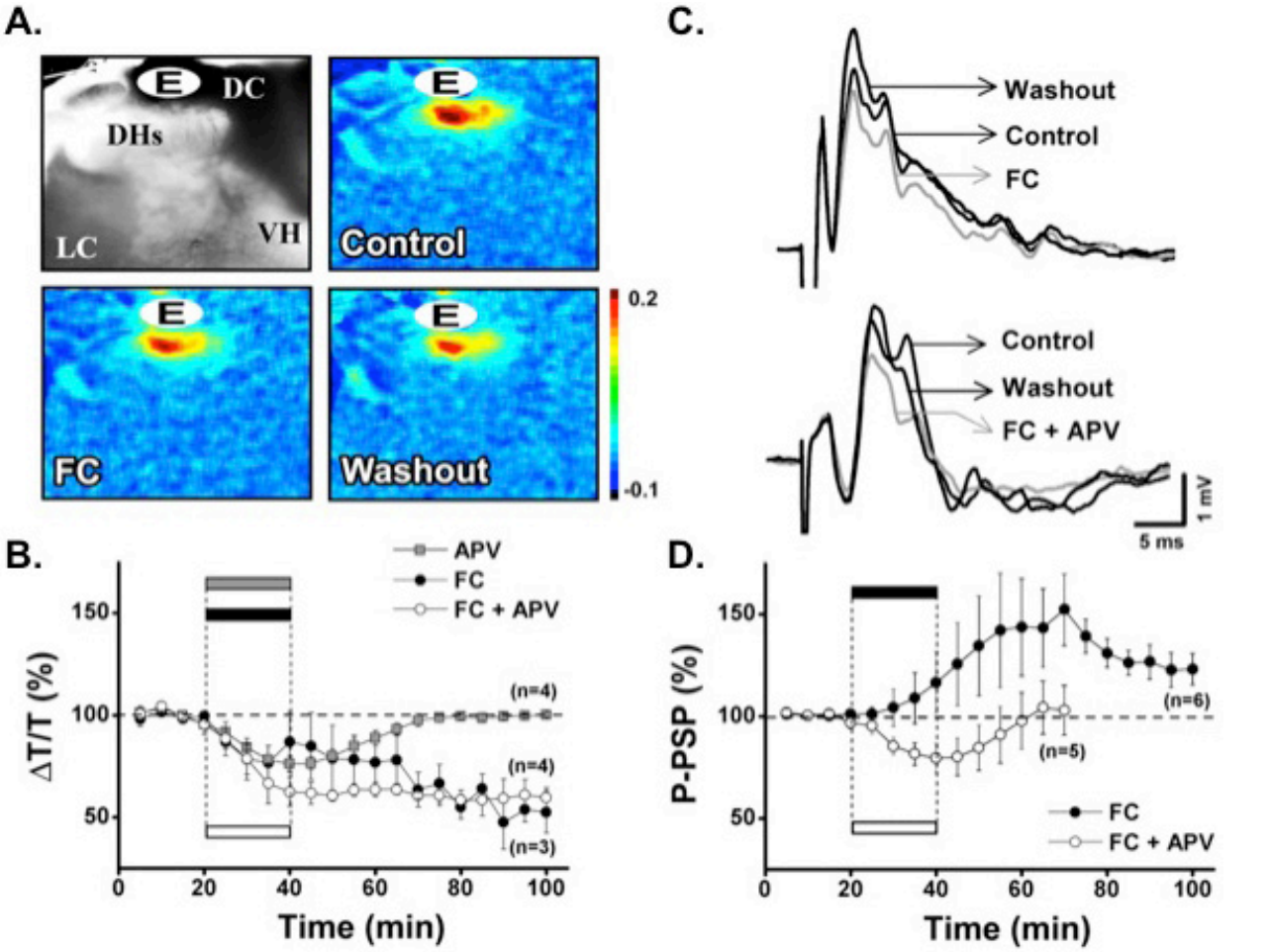

Fig. 1. FC modification of the optical and neuronal responses of the DH_s. (A) Effect of FC on the optical intrinsic signal (OIS_{DR}). Reference image (grayscale) showing location of stimulating electrode (E) and anatomical regions within the image field - superficial dorsal horn (DH_s); dorsal column (DC); ventral horn (VH); and lateral column (LC). Colour scale at right indicates OIS_{DR} intensity (ΔT/T×100) and applies to each average difference (prestimulus - poststimulus) image (Control, FC, and Washout). (B) Time course of effect on OIS_{DR} of 50 μM FC (filled circles), 50 μM FC+50 μM APV (open circles), and 50 μM APV (gray squares). (C) Average across-trial field potential (average P-PSP_{DR} to 10 stimuli) recorded from DH_s during control, exposure to FC, and washout periods. (D) Time course of effect on P-PSP_{DR} of 50 μM FC (filled circles) *vs.* 50 μM FC+50 μM APV (open circles). Each point indicates amplitude of potential averaged across ten consecutive trials. Horizontal bars in B and D identify 20 min period slice was exposed to each treatment; error bars=±1SE.

http://dx.doi.org/10.5607/en.2014.23.1.53

(orange trace - FC) is slightly smaller than the potential recorded prior to the exposure to FC (black trace - Control), the $P\text{-}PSP_{DR}$ recorded after restoration of the perfusion solution to drug-free normal ACSF (red trace - Washout) is substantially larger than the $P\text{-}PSP_{DR}$ recorded prior to the exposure to FC.

Fig. 1D shows the average across-slice (n=6) time course of the effect of FC on the $P\text{-}PSP_{DR}$ (plot with filled circles). In each of 6 slices studied in this way exposure to FC was followed (during the initial 20~35 min of the 60 min washout period) by a substantial increase in $P\text{-}PSP_{DR}$ amplitude (the peak increase in the $P\text{-}PSP_{DR}$ during washout ranged between 140~168%; mean=153%; n=6). Over the last 30~35 min of the washout period $P\text{-}PSP_{DR}$ magnitude declined progressively, but in no slice did $P\text{-}PSP_{DR}$ amplitude return to values measured prior to FC exposure ($P\text{-}PSP_{DR}$ amplitude at the end of the 60 min washout period was 115~132% of Control; mean=124%; n=6).

Similar to the findings reported in previous studies of the long-term effects of repetitive afferent drive on glutaminergic neurotransmission at a variety of sites in the CNS (e.g., spinal cord dorsal horn - [3]; hippocampus - [23-25]; neocortex - [26, 27]), LTP_{FC} apparently requires NMDA receptor activation because no facilitation of DH_s excitatory neurotransmission occurred when APV (at a concentration that achieves a nearly complete block of NMDA receptors; 50 μM; plot with open circles at Fig. 1D; n = 5) was present in the perfusion solution during the time the slice was exposed to FC. In contrast, FC's suppression of the OIS_{DR} apparently does not require NMDA receptor activation because exposure to APV+FC (plot with open circles at Fig. 1B) failed to significantly alter either the magnitude or time course of the reduction of the OIS_{DR} that followed exposure to FC. Consistent with the demonstration that magnitude of the OIS_{DR} depends on glutamatergic neurotransmission [4, 21], APV application alone led to a modest suppression of the OIS_{DR} (plot with gray squares at Fig. 1B) that reversed and returned to control levels 20~25 min after the perfusion solution was restored to drug-free, normal ACSF.

The possibility that excess local accumulation of K^+ in the DH_s might, at least in part, be responsible for FC's long-term alteration of DH_s excitatory neurotransmission was evaluated by varying (from one slice to the next) the $[K^+]_o$ in the perfusion solution during the exposure to FC. The plots of $P\text{-}PSP_{DR}$ magnitude vs. time in Fig. 2A show that the effect of the exposure to FC modified strikingly and systematically as $[K^+]_o$ in the perfusion solution (and, therefore, in the DH_s) was varied over the range 3.0~0.0 mM. Reduction of K^+ in the ACSF by 1 mM (i.e., to 2 mM; plot with open squares in Fig. 2A) eliminated the long-term enhancement of DH_s neurotransmission detected when FC was provided to the slice in normal ACSF. Moreover, when $[K^+]$ in the perfusate

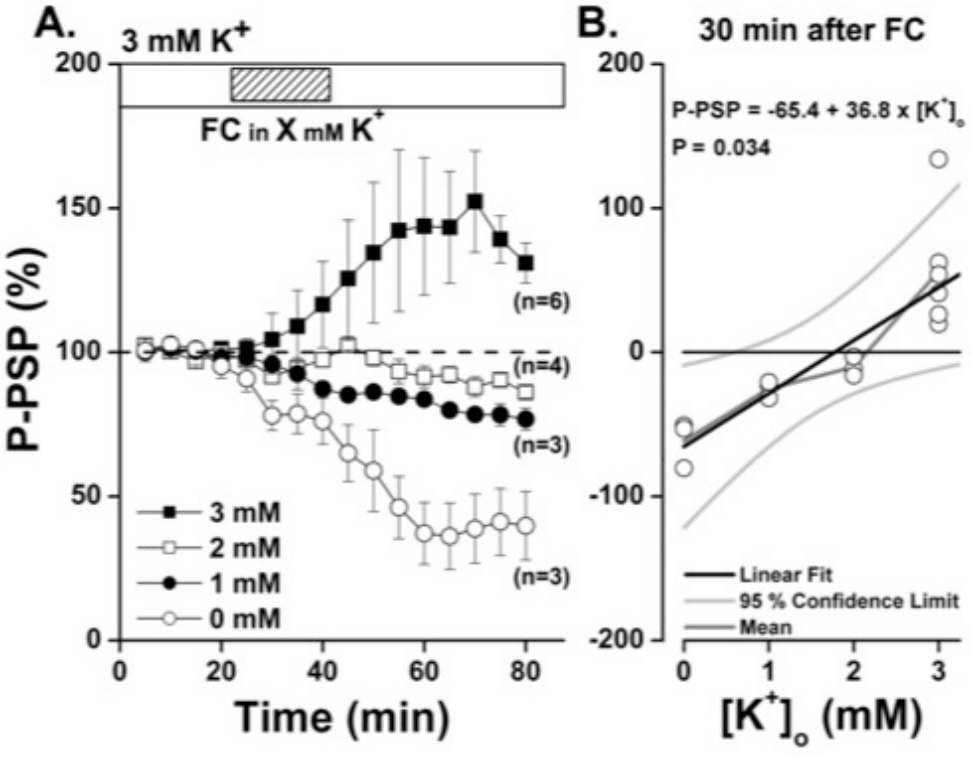

Fig. 2. Dependency on K^+_o of FC-induced modification of DH_s neurotransmission. (A) Plots showing that effect of FC on the $P\text{-}PSP_{DR}$ alters systematically as $[K^+]_o$ is varied over the range 0~3 mM. Format same as Fig. 1B. (B) Linear regression analysis of the relationship between magnitude of FC-induced alteration of $P\text{-}PSP_{DR}$ and $[K^+]_o$ revealing that over the range 0~3 mM a 1 mM change of $[K^+]_o$ is accompanied by nearly a 37% alteration of DH_s neuron responsivity. Note that at $[K^+]_o$ values less than 1.8 mM FC induces LTD; however, at values exceeding 1.8 mM FC induces LTP.

was 1 mM or less, exposure to FC was followed by a long-term depression of the P-PSP$_{DR}$ (LTD$_{FC}$; plots with filled and open circles). Statistical analysis of the data obtained from each slice and under each condition at 30 min after exposure to FC revealed that the $[K^+]_o$ dependency of FC's effect on the magnitude of the DH$_s$ response to small-diameter afferent drive is linear and statistically significant (Fig. 2B; p=0.034; P-PSP$_{DR}$=-65.4+36.8×$[K^+]_o$; X-intercept=1.8 mM $[K^+]_o$).

A third and final series of field potential recording experiments was carried out to determine if manipulation of $[K^+]_o$ in the perfusion solution would modify the long-term potentiation of DH$_s$ excitatory neurotransmission that develops in normal ACSF (containing 3.0 mM $[K^+]_o$) following an exposure to FC. The result obtained from every slice (n = 4) studied in this way was consistent and unambiguous (Fig. 3) - that is, at the time at which the effect of FC on the P-PSP$_{DR}$ was maximal (at 30 min after the exposure to FC) switch of the perfusion solution to ACSF containing zero K^+ was accompanied by a rapid decrease of the P-PSP$_{DR}$ to pre-FC (control) values. Clearly, therefore, DH$_s$ excitatory neurotransmission remained exquisitely sensitive to $[K^+]_o$ after the exposure to FC.

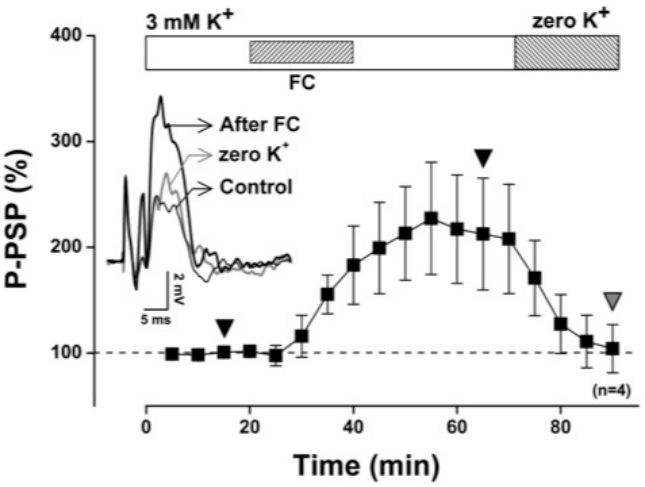

Fig. 3. Lowering $[K^+]_o$ eliminates the LTP that follows exposure to FC. Inset - superimposed average DH$_s$ field potentials (P-PSP$_{DRs}$; each trace shows the average response to 10 stimuli) recorded from same DH$_s$ site during the control period (at 15 min after the start of recording), and at 60 and 90 min (indicated by arrowheads), respectively. Shaded regions in horizontal bar at top indicate exposures to FC and zero K^+; slice was exposed to ACSF containing 3 mM K^+ during initial 70 min of the study.

The superimposed field potential recordings at the top left of Fig. 4A illustrate a prominent characteristic of field potential recordings obtained from the medial DH$_s$ (e.g., see [28], also [11]) - that is, high-frequency and rhythmic postsynaptic neuronal activation is apparent in the response to dorsal root stimulation (gray trace for the 3 conditions - control, after FC, and zero K^+), as well as in across-trial (n = 10) averages of the DH$_s$ response obtained under the same conditions (black traces). Inspection of the single-trial and average across-trial responses recorded under the 3 conditions shows that: (1) exposure to FC not only is followed by a large increase in the magnitude of the average across-trial DH$_s$ field potential (LTP$_{FC}$), but also by a prominent increase in the synchronous, high-frequency DH$_s$ activation observable in the response to each stimulus; and (2) both the LTP$_{FC}$ and the increased high-frequency activation induced by FC are substantially reduced when the solution perfusing the slice is switched to ACSF containing zero K^+.

FFT analysis of the single-trial responses (histograms on Fig. 4B) quantitatively confirmed that: (1) FC exposure was followed by a prominent increase of the synchronized, high-frequency component of the DH$_s$ response to the dorsal root stimulus; and (2) perfusion of the slice with ACSF containing zero K^+ eliminated the enhancement of the high-frequency component that occurred following the exposure to FC. The pseudocolour 3-D plot (upper part) and surface projection map (lower part) in Fig. 4C illustrate (for the same slice that yielded the responses in Fig. 4A) the characteristic temporal attributes of the high-frequency DH$_s$ activation evoked by a dorsal root stimulus following exposure to FC - i.e., multiple peaks in the DH$_s$ field potential; neighboring peaks separated by a 5~8 msec interval during which voltage was at or near-baseline.

The recently published demonstration that GABA$_A$ receptor block reverses the injury-induced sensitization of nociceptor-specific neurons in the DH$_s$ of intact animals [14], together with the proposal [13] that GABA becomes a postsynaptic excitatory neurotransmitter in the DH$_s$ following peripheral nerve injury motivated us to evaluate the impact, if any, of GABA$_A$ receptor block on the LTP induced by FC. Panel A in Fig. 5 shows field potential recordings (P-PSP$_{DRs}$) obtained from the ipsilateral DH$_s$ of an exemplary subject before ("Control"), 30 min after bath application of FC ("after FC"; revealing a prominent LTP$_{FC}$) and, finally, 30 min after exposure of the same slice to ACSF containing 20 μM bicuculline ("after Bic"; revealing that after exposure to Bic the LTP induced by FC was no longer evident). The plot in panel B shows the time course of the effect of Bic on the LTP induced by exposure to FC (average of data obtained from 4 slices studied in the same way). These findings reveal that LTP$_{FC}$ depends on GABA$_A$ receptor-mediated neurotransmission because, like its effect on the dorsal horn sensitization induced by application of algesic chemical to the receptive field [14], the GABA$_A$ receptor block achieved by Bic antagonizes the LTP induced by exposure to FC.

http://dx.doi.org/10.5607/en.2014.23.1.53

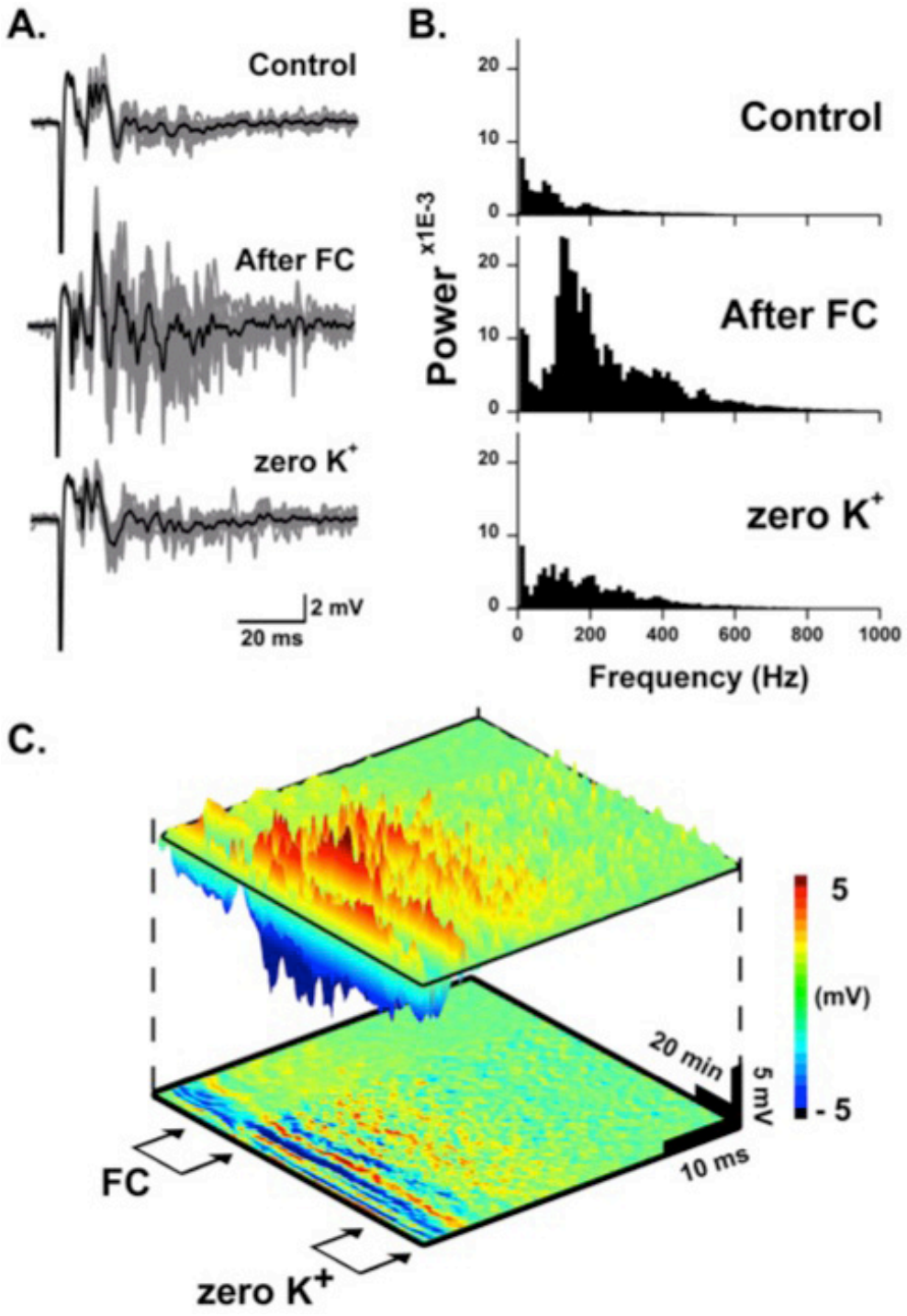

Fig. 4. Effect of FC on the temporal properties of the DH_s response to dorsal root stimulation. (A) Superimposed across-trial (average response to 10 stimuli - black trace) and single-trial responses (gray traces) of DH_s to dorsal root stimulation. Recordings were obtained during the control period (top), 20 min after exposure to FC (middle), and subsequently (bottom) after switch of the perfusion solution to ACSF containing zero K^+. (B) Average power spectra computed for all responses (n = 40) obtained during control, after FC, and zero $[K^+]_o$ periods. (C) 3D- (top) and surface projection (bottom) maps showing a) synchronous, high-frequency DH_s neuronal activation induced by exposure to FC when $[K^+]_o$ in the ACSF was 3 mM, and b) suppression of the FC-induced high-frequency activation following switch of the perfusion solution to ACSF containing 0 mM K^+.

Cellular-level observations-

Effects of FC on the DH_s neuron response to GABA

The current vs. time traces in Fig. 5B show the transmembrane currents evoked at different holding potentials in a representative DH_s neuron in response to the a brief increase in the local concentration of GABA ("puff"), both before ("Control", top left) and after (FC; top right) a 20 min exposure of the slice to 50 μM FC. The I-V curves shown as insets below the traces in Fig. 5B demonstrate that while the relationship between GABA-evoked peak current and membrane potential is essentially linear both before and after FC, the X-intercept of the best-fitting linear regression line (indicating the equilibrium potential for the ionic currents triggered by GABA - E_{GABA}) for the observations obtained after the exposure to FC (approx. -50 mV) is substantially more

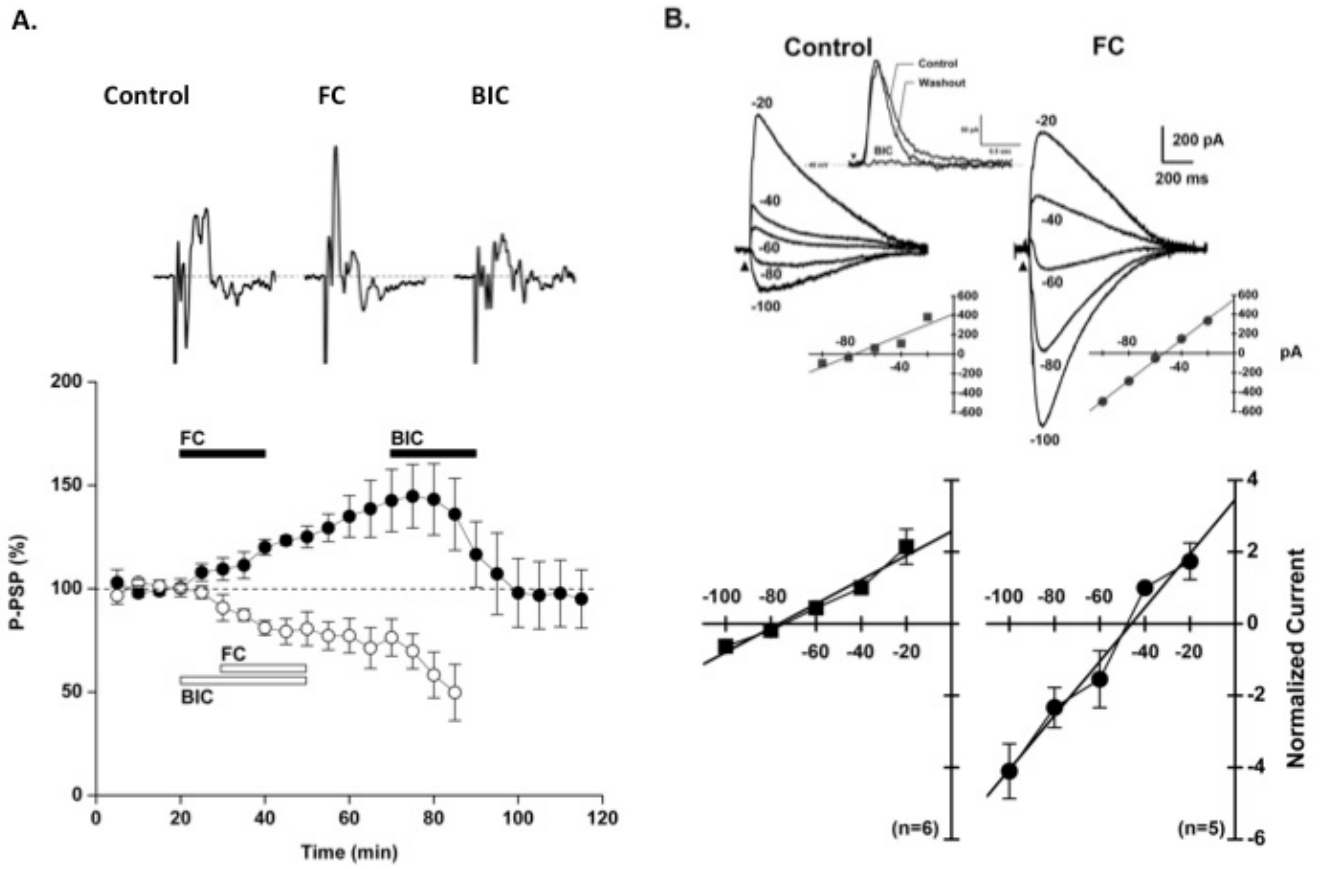

Fig. 5. Effect of FC on E_{GABA}. (A) Average of five consecutive field potentials evoked in DH_s by dorsal root stimulus before ("Control"), 10 min after exposure to FC ("after FC"), and after exposure to ACSF containing 20 μM Bic ("after Bic"). Plot showing average across-slice (n=4) effect of Bic application on LTP associated with exposure to FC. (B) Upper panel shows GABA puff-evoked currents recorded from DH_s neuron before and after exposure to FC. A 300 msec puff of 1 mM GABA was applied at each of the indicated holding potentials. E_{GABA} prior to FC was approx. -75 mV; E_{GABA} 20 min after FC was approx. -50 mV. Current-voltage (IV) plots derived from observations obtained from same neuron shown under voltage clamp recordings. Lower panel shows Plot of normalized average across-neuron I-V plot obtained before (on left; n=6) and after exposure to FC (on right; n=5). Normalization procedure: current measured from each neuron at each holding potential is expressed in terms of the current measured from same neuron/condition at -40 mV. Estimates X-intercept of best fitting linear regression line is -76.5 mV for observations obtained before FC, and -46.1 mV after FC. Flags indicate ±1 S.E.M.

positive than the X-intercept for the data obtained prior to FC (approx. -75 mV).

The lower left and right panels of Fig. 5B show I-V curves obtained by averaging the data obtained from 5 neurons studied using the above-described protocol (enabling measurement of peak transmembrane current evoked in each neuron before and after exposure to FC by GABA application at holding potentials stepped between -20 and -100 mV). As was the case for the neuron that provided the data in Fig. 5B (upper), both the across-neuron (n=5) before-FC (on the left; Fig. 5B) and after-FC (on the right; Fig. 5B) I-V curves are well-fit by linear regression lines ($p<.002$), and the X-intercept (indicating E_{GABA}) for the post-FC observations is substantially and statistically different ($p<.001$) from the X-intercept for the pre-FC observations (exposure to FC is associated with a substantial depolarizing alteration - approximately 31 mV - of E_{GABA}; i.e, E_{GABA} changes from -76.5 mV preFC to -46.1 mV postFC). Interestingly (see Discussion), the slope of the regression line for the observations obtained subsequent to FC is significantly larger ($p<.003$) than the slope of the best fitting line for the data obtained prior to FC.

DISCUSSION

Role of glia in long-term plasticity-

Long-term enhancement of excitatory neurotransmission between small-diameter nociceptive afferents and the DH_s neurons that receive their synaptic terminals (LTP) is regarded as the primary neural mechanism that underlies central sensitization

http://dx.doi.org/10.5607/en.2014.23.1.53

and the associated abnormalities of pain perception, including hyperalgesia, allodynia, and persistent pain [3, 29]. Given the use-dependent nature of LTP [24, 25], it is understandable that most studies have employed high-frequency afferent conditioning stimulation to induce it. Nevertheless, the demonstration [2] that LTP can be induced by spinal application of agents that evoke spike activity in DH_s neurons makes it clear that presynaptic activity is not essential for LTP induction at the initial stage of the CNS pathways that process information about the status of peripheral nociceptors. Instead, the observations obtained in the present study make it likely [3] that LTP can result from the extrasynaptic spread of neuroactive compounds synthesized and released by DH_s neurons or glia.

Mechanisms of glial-initiated long-term plasticity-

Although astrocytes normally function as "active partners" in CNS neurotransmission [30], a variety of evidence indicates that under a variety of pathological conditions (peripheral inflammation, injury, infection) their contributions can become maladaptive. The finding that nerve injury is accompanied by trans-synaptic reduction in the neuronal expression of the potassium-chloride exporter KCC2 - an alteration that disrupts lamina I neuron anion homeostasis - is notable in this regard because it raises the possibility that abnormal dorsal horn glia-neuron interactions can contribute to hyperalgesia / persistent pain [13]. Coull et al. (2003) demonstrated that DH_s lamina I neuron expression of KCC2 is decreased after nerve injury - an outcome that results in the intracellular accumulation of Cl^- in lamina I neurons which, in turn, shifts the Cl^- equilibrium potential in a depolarizing direction and, in this way, converts the postsynaptic action of GABA from hyperpolarizing (inhibitory) to depolarizing (excitatory). As a result, after nerve injury DH_s neurons exhibit abnormal excitability including a novel responsivity to peripheral stimuli that evoke activity in A_β afferents [13, 14, 31]. Although comparable studies of DH_s neurons remain to be carried out, Fiumelli et al. (2005) have demonstrated that repetitive postsynaptic spiking of hippocampal neurons leads (within minutes) to a Ca^{2+}-dependent downregulation of KCC2 expression, a depolarizing shift of E_{GABA} and, as a consequence, the effect of GABA converts from inhibition to excitation [32].

Although significant gaps (such as the effect of spike activity on KCC2) remain to be addressed, the findings obtained in the present study significantly extend current views of the mechanisms by which DH_s excitatory neurotransmission undergoes modification. First, they demonstrate that the elevation of local $[K^+]_o$ that occurs in the DH_s subsequent to inhibition of astrocyte energy metabolism by FC is accompanied by a depolarizing shift in the E_{GABA} of DH_s neurons (Fig. 5B) - a shift which converts the effect of the transmembrane ionic currents associated with $GABA_A$ receptor activation convert from hyperpolarizing (inhibitory) to depolarizing (excitatory). Second, the observations obtained in the present study reveal that exposure to FC is accompanied by a significant increase in the slope of the relationship between membrane potential and the transmembrane current evoked by GABA (Fig. 5B) - an outcome indicating that DH_s neurons exhibit a larger GABA-mediated membrane conductance to Cl^- after exposure to FC (compare current traces obtained before and after FC; Fig. 5B).

The prominent suppression of the OIS_{DR} that reliably follows exposure to FC (Fig. 1) is fully consistent with the proposal that astrocytes are the major source of the tissue transmittance increase that underlies the intrinsic optical signal (OIS_{DR}) evoked in the DH_s by dorsal root stimulation (reviewed in [4, 33, 34]). Such an effect of FC, taken together with the report [5] that in normal subjects $[K^+]_o$ is maintained at lower values in the superficial dorsal horn (laminae I-II) than in the deeper laminae (laminae III-V), raises the functionally intriguing possibility that the capacity of astocytes to remove excess extracellular K^+ (as well as glutamate and other neuroactive substances) is substantially greater in the DH_s than in the deeper layers of the horn.

A DH_s control mechanism involving astrocyte-neuron interactions-

Although additional evidence will be required to confirm its validity, the view which guides our ongoing investigation of DH_s glial-neural interactions is that astrocytes are part of a DH_s control mechanism which, in normal subjects, permits relatively rapid and effective adjustment (accomplished via stimulus-directed astroctye-neuron interactions) of DH_s neuron excitability/ responsivity at this initial stage of CNS nociceptive information processing. The contributions to both normal and abnormal sensory function of such a control mechanism are regarded as potentially significant. More specifically, although the normally highly efficient astrocyte regulation of $[K^+]_o$ in the DH_s ensures the maintenance of a relatively low (presumably desirable) level of excitability at this initial level of the CNS "pain" projection path, the slow (relative to stimulus-driven neuronal activity) temporal characteristics of DH_s astrocyte-mediated uptake and release of K^+ and other neuroactive substances may contribute importantly to experience-driven and functionally-adaptive modulation of DH_s neuron responsivity (e.g., these properties of DH_s astrocytes may enable astrocytes to modify the "wind-up" behavior of DH_s neurons). Finally, a vigorous episode of nociceptor afferent input (e.g., that evoked by intracutaneous injection of algesic

chemical; [4]) is viewed to make this control system maladaptive by interfering with the ability of DH_s astrocytes to regulate extracellular K^+ and glutamate which, as demonstrated by the experimental findings described in this paper, triggers a long-term enhancement of DH_s excitatory neurotransmission (LTP) which in a conscious subject, would be accompanied by perceptual abnormalities such as hyperalgesia, allodynia, and persistent pain.

Concepts of glia involvement in spinal cord nociceptive information processing-

Multiple animal behavioral studies have used FC to assess the role of glia in the hyperalgesia that occurs following manipulations such as intracutaneous injection of algesic chemical (e.g, formalin - [35]; zymosan - [36]), tetanic electrical stimulation of a peripheral nerve at C-fibre strength [37, 38], or perisciatic application of agents that evoke immune activation [39]. Such studies have consistently reported that direct application of FC to the spinal cord (e.g., at 10 min - 1 hr before performance of the manipulation used to elicit hyperalgesia) at a dose that inhibits glial energy metabolism via the TCA cycle prevents or greatly attenuates the hyperalgesia - and this effect of FC has uniformly interpreted to indicate that the FC inhibition of glial metabolism prevents the glial release of a variety of factors critical for the excessive activation of dorsal horn neurons that underlies hyperalgesia.

This interpretation appears directly at odds with this study's finding that transient exposure to FC induces a long-term *enhancement* of excitatory neurotransmission in the superficial spinal cord dorsal horn. Consideration of our observations in the context of those reported in a recent study of hippocampal neuron-astrocyte metabolic interaction [40], however, suggests an alternative and, at least to date, not previously considered explanation for the finding that spinal pre-administration of FC prevents/attenuates the hyperalgesia induced by intracutaneous injection of algesic chemical, peri-sciatic immune activation, or tetanic stimulation of C-fibre afferents. That is, Bacci et al. (2002) found that exposure to FC not only inhibits astrocyte energy production via the TCA cycle, but also leads FC-intoxicated astrocytes to use glutamine as an alternative energy source, enabling astrocyte ATP levels to be maintained near-to-normal for hours (for concise review of effects of FC on astrocyte energy metabolism see [40]). As a result, as astrocyte release of glutamine declines in the presence of FC, primary afferent nerve terminals become deprived of the glutamine required to maintain the efficacy of excitatory glutaminergic neurotransmission between nociceptive afferents and DH_s neurons, dorsal horn nociceptive information processing fails, and pain perception diminishes. Accordingly, although behavioral studies have shown that prior FC application to the spinal cord prevents/attenuates hyperalgesia, this effect of FC may not be attributable (as has been widely assumed) to astrocyte release of neuroactive substances, but instead may be the result of a decreased availability of astrocytic glutamine for conversion to glutamate in primary nociceptive afferent terminals (via the glutamine-glutamate cycle; [4, 40, 41]). The rapid onset of the DH_s neuron LTP that occurs after washout of FC is regarded as consistent with this interpretation. In addition, our finding that LTP_{FC} is reduced/eliminated by lowering K^+ in the solution perfusing the slice (Fig. 2) is viewed to indicate that DH_s $[K^+]_o$ increases when astrocyte metabolism is inhibited, and contributes importantly (via direct actions on neurons and/or by enhancing NMDA receptor activity) to the long-term enhancement of DH_s excitatory neurotransmission observed subsequent to exposure to FC.

COMPETING INTERESTS

The authors declare that they have no competing interest.

AUTHORS' CONTRIBUTIONS

JL, OF, MT, and BW conceived of the project and designed experiments. JL performed all experiments, analyzed data. JL, CJL, and BW wrote the manuscript. All authors read and approved the manuscript.

ACKNOWLEDGEMENTS

The experiments were funded by NIH grant NS037501 (B. Whitsel, P.I.). M. Tommerdahl was supported, in part, by NIH grant NS050587 (M. Tommerdahl, P.I.). The authors thank Betsy Houston for technical assistance and P.M. Quibrera for help with statistical analyses.

REFERENCES

1. Ikeda H, Stark J, Fischer H, Wagner M, Drdla R, Jäger T, Sandkühler J (2006) Synaptic amplifier of inflammatory pain in the spinal dorsal horn. Science 312:1659-1662.
2. Liu XG, Sandkühler J (1998) Activation of spinal N-methyl-D-aspartate or neurokinin receptors induces long-term potentiation of spinal C-fibre-evoked potentials. Neuroscience 86:1209-1216.
3. Sandkühler J (2000) Learning and memory in pain pathways. Pain 88:113-118.
4. Lee J, Tommerdahl M, Favorov OV, Whitsel BL (2005)

http://dx.doi.org/10.5607/en.2014.23.1.53

Optically recorded response of the superficial dorsal horn: dissociation from neuronal activity, sensitivity to formalin-evoked skin nociceptor activation. J Neurophysiol 94:852-864.
5. Svoboda J, Motin V, Hájek I, Syková E (1988) Increase in extracellular potassium level in rat spinal dorsal horn induced by noxious stimulation and peripheral injury. Brain Res 458:97-105.
6. Fleck MW, Palmer AM, Barrionuevo G (1992) Potassium-induced long-term potentiation in rat hippocampal slices. Brain Res 580:100-105.
7. Pascual O, Casper KB, Kubera C, Zhang J, Revilla-Sanchez R, Sul JY, Takano H, Moss SJ, McCarthy K, Haydon PG (2005) Astrocytic purinergic signaling coordinates synaptic networks. Science 310:113-116.
8. Yang Y, Ge W, Chen Y, Zhang Z, Shen W, Wu C, Poo M, Duan S (2003) Contribution of astrocytes to hippocampal long-term potentiation through release of D-serine. Proc Natl Acad Sci U S A 100:15194-15199.
9. Ge WP, Duan S (2007) Persistent enhancement of neuron-glia signaling mediated by increased extracellular K+ accompanying long-term synaptic potentiation. J Neurophysiol 97:2564-2569.
10. Fonnum F, Johnsen A, Hassel B (1997) Use of fluorocitrate and fluoroacetate in the study of brain metabolism. Glia 21:106-113.
11. Willoughby JO, Mackenzie L, Broberg M, Thoren AE, Medvedev A, Sims NR, Nilsson M (2003) Fluorocitrate-mediated astroglial dysfunction causes seizures. J Neurosci Res 74:160-166.
12. Watkins LR, Maier SF (2002) Beyond neurons: evidence that immune and glial cells contribute to pathological pain states. Physiol Rev 82:981-1011.
13. Coull JA, Boudreau D, Bachand K, Prescott SA, Nault F, Sík A, De Koninck P, De Koninck Y (2003) Trans-synaptic shift in anion gradient in spinal lamina I neurons as a mechanism of neuropathic pain. Nature 424:938-942.
14. Garcia-Nicas E, Laird JM, Cervero F (2006) GABAA-receptor blockade reverses the injury-induced sensitization of nociceptor-specific (NS) neurons in the spinal dorsal horn of the rat. J Neurophysiol 96:661-670.
15. Hantman AW, van den Pol AN, Perl ER (2004) Morphological and physiological features of a set of spinal substantia gelatinosa neurons defined by green fluorescent protein expression. J Neurosci 24:836-842.
16. Lu Y, Perl ER (2003) A specific inhibitory pathway between substantia gelatinosa neurons receiving direct C-fiber input. J Neurosci 23:8752-8758.
17. Ruscheweyh R, Sandkühler J (2000) Differential actions of spinal analgesics on mono-versus polysynaptic Adelta-fibre-evoked field potentials in superficial spinal dorsal horn in vitro. Pain 88:97-108.
18. Asai T, Kusudo K, Ikeda H, Takenoshita M, Murase K (2002) Effect of halothane on neuronal excitation in the superficial dorsal horn of rat spinal cord slices: evidence for a presynaptic action. Eur J Neurosci 15:1278-1290.
19. Ikeda H, Heinke B, Ruscheweyh R, Sandkühler J (2003) Synaptic plasticity in spinal lamina I projection neurons that mediate hyperalgesia. Science 299:1237-1240.
20. Murase K, Saka T, Asai T, Ikeda H (1999) Functional circuitry for the induction of prolonged excitation in the rat spinal dorsal horn. Eur J Neurosci 11:3355-3358.
21. Murase K, Saka T, Terao S, Ikeda H, Asai T (1998) Slow intrinsic optical signals in the rat spinal dorsal horn in slice. Neuroreport 9:3663-3667.
22. Ruscheweyh R, Sandkühler J (2001) Bidirectional actions of nociceptin/orphanin FQ on A delta-fibre-evoked responses in rat superficial spinal dorsal horn in vitro. Neuroscience 107:275-281.
23. Bliss TV, Collingridge GL (1993) A synaptic model of memory: long-term potentiation in the hippocampus. Nature 361:31-39.
24. Linden DJ (1999) The return of the spike: postsynaptic action potentials and the induction of LTP and LTD. Neuron 22:661-666.
25. Malenka RC (1994) Synaptic plasticity in the hippocampus: LTP and LTD. Cell 78:535-538.
26. Artola A, Singer W (1987) Long-term potentiation and NMDA receptors in rat visual cortex. Nature 330:649-652.
27. Rioult-Pedotti MS, Friedman D, Donoghue JP (2000) Learning-induced LTP in neocortex. Science 290:533-536.
28. Ruscheweyh R, Sandkühler J (2003) Epileptiform activity in rat spinal dorsal horn in vitro has common features with neuropathic pain. Pain 105:327-338.
29. Woolf CJ, Salter MW (2000) Neuronal plasticity: increasing the gain in pain. Science 288:1765-1769.
30. Newman EA (2003) New roles for astrocytes: regulation of synaptic transmission. Trends Neurosci 26:536-542.
31. Torsney C, MacDermott AB (2006) Disinhibition opens the gate to pathological pain signaling in superficial neurokinin 1 receptor-expressing neurons in rat spinal cord. J Neurosci 26:1833-1843.
32. Fiumelli H, Cancedda L, Poo MM (2005) Modulation of GABAergic transmission by activity via postsynaptic Ca2+-

dependent regulation of KCC2 function. Neuron 48:773-786.
33. Lee J, Woo J, Favorov OV, Tommerdahl M, Lee CJ, Whitsel BL (2012) Columnar distribution of activity dependent gabaergic depolarization in sensorimotor cortical neurons. Mol Brain 5:33.
34. Whitsel BL, Favorov OV, Li Y, Lee J, Quibrera PM, Tommerdahl M (2010) Nociceptive afferent activity alters the SI RA neuron response to mechanical skin stimulation. Cereb Cortex 20:2900-2915.
35. Watkins LR, Martin D, Ulrich P, Tracey KJ, Maier SF (1997) Evidence for the involvement of spinal cord glia in subcutaneous formalin induced hyperalgesia in the rat. Pain 71:225-235.
36. Meller ST, Dykstra C, Grzybycki D, Murphy S, Gebhart GF (1994) The possible role of glia in nociceptive processing and hyperalgesia in the spinal cord of the rat. Neuropharmacology 33:1471-1478.
37. Ma JY, Zhao ZQ (2002) The involvement of glia in long-term plasticity in the spinal dorsal horn of the rat. Neuroreport 13:1781-1784.
38. Ying B, Lü N, Zhang YQ, Zhao ZQ (2006) Involvement of spinal glia in tetanically sciatic stimulation-induced bilateral mechanical allodynia in rats. Biochem Biophys Res Commun 340:1264-1272.
39. Chacur M, Milligan ED, Gazda LS, Armstrong C, Wang H, Tracey KJ, Maier SF, Watkins LR (2001) A new model of sciatic inflammatory neuritis (SIN): induction of unilateral and bilateral mechanical allodynia following acute unilateral peri-sciatic immune activation in rats. Pain 94:231-244.
40. Bacci A, Sancini G, Verderio C, Armano S, Pravettoni E, Fesce R, Franceschetti S, Matteoli M (2002) Block of glutamate-glutamine cycle between astrocytes and neurons inhibits epileptiform activity in hippocampus. J Neurophysiol 88:2302-2310.
41. Largo C, Cuevas P, Somjen GG, Martín del Río R, Herreras O (1996) The effect of depressing glial function in rat brain in situ on ion homeostasis, synaptic transmission, and neuron survival. J Neurosci 16:1219-1229.

http://dx.doi.org/10.5607/en.2014.23.1.53